ICAS 2016
30th Congress of the International Council of the Aeronautical Sciences
DCC, Daejeon, Korea ; September 25-30, 2016

HYBRID-ELECTRIC MOTIVE POWER SYSTEMS FOR COMMUTER TRANSPORT APPLICATIONS

Yann Fefermann, Christophe Maury, Clélia Level, Khaled Zarati, Jean-Philippe Salanne, Clément Pornet, Bruno Thoraval, Askin T. Isikveren
SAFRAN S.A., Magny-Les-Hameaux, 78772, France

Keywords: *hybrid-electric, propulsion, systems architecture, aircraft design*

Abstract

This investigation surveyed the potential and established outcomes for future 19-passenger fixed-wing commuter transport aircraft concepts employing battery based Voltaic-Joule/Brayton motive power systems with no additional electrical energy drawn from generators mechanically coupled to thermal engines. The morphological approach was that of a tri-prop (two on-wing podded turbo-props and one aft-fuselage mounted electric motor configured as a pusher-on-pylon installation). A Battery System-level Gravimetric Specific Energy (referred to as "battery energy density") of at least 500 Wh/kg yielded 39%, 25% and 10% block fuel reductions for 150 nm (Design Service Goal), 430 nm (85-percentile) and 700 nm (maximum range) stage lengths respectively. All quoted comparisons are against a suitably projected turbo-prop only year-2030 aircraft. In contrast to the reference Beech 1900D, block fuel reductions of up to 44-49% were predicted, which could facilitate a significantly lower deficit in relation to the ACARE Strategic Research and Innovation Agenda 55% target for year 2030. This investigation also indicated that, in future, suitably flexible hybrid-electric architectures could be fashioned allowing possibility for the aircraft to complete any required city-pair operations (within the legitimate payload-range working capacity) irrespective of exchangeable batteries being available at a given station. Finally, it was also established assuming such a tri-prop morphology Normal Conducting Machines delivering maximum shaft power output of 1.1 MW would be required.

Nomenclature

Symbol	Description	Unit
AGB	Accessory Gear Box	-
Batt	Battery	-
BC	Battery Controller	-
Ctlr	Controller	-
E	Energy	kWh
Elec	Electrical	-
F_B	Fuel Burn	kg
FH	Flight Hours	h
F_N	Reference Thrust	N
GA	Go-Around	-
M/G	Motor/Generator	-
OEI	One Engine Inoperative	-
P	Power	kW
Red.	Reduction gearbox	-
STD	Standard Deviation	-
Th	Thermal	-
T/O	Take-Off	-

1 Introduction

The primary aim of deploying hybrid-electric technologies on aircraft is to seek pragmatic, appropriately projected engineering solutions in meeting aggressive emissions and noise targets declared by the European Commission [1], the US National Aeronautics and Space Administration (NASA), the International Air Transport Association and the International Civil Aviation Organization. In the context of this technical paper the term "hybrid-electric" covers concepts that employ some form of parallel and/or serial combinatorial power-train arrangement that utilizes a kerosene based thermal engine and batteries only as the main

source of energy for advanced electrical motor(s). The resulting arrangement is referred to here as Voltaic-Joule/Brayton (VJB) motive power systems.

Previously published investigations [2-10] focused on the conceptual design and discussion of parametric sensitivities associated with hybrid-electric motive power systems for commercial aircraft accommodating 50-180 PAX servicing short-haul operations and targeting year entry-into-service (EIS) of 2035+. Upon declaration of a dual objective comprising relative block fuel reduction and operating economics, and, after comparing and contrasting the relative merits of several "wing-and-tube" compatible propulsion system layouts it was concluded in Ref. [2] that a "distributed parallel" tri-fan configuration comprising two under-wing podded gas-turbines and one advanced Normal Conducting Motor mounted in the aft-fuselage as an S-duct installation could be an appropriate morphological choice. The research outcome also provided tell-tale signs that smaller scale commercial transports can be construed as being the "critical design case". This means as current industry research and development activities focus on smaller aircraft types pragmatic technical solutions fashioned for this class of aircraft will serve to become a favorable "fall-out" as larger scale aircraft are considered in the future.

1.1 Parametric Descriptor Convention, Figures-of-Merit and Synthetic Objectives

The degree-of-hybridization employed in advanced VJB based motive power systems cannot be suitably represented by a single parametric descriptor. As argued in Ref. [2] a full description of any generic hybrid Propulsion and Power System (PPS) requires two descriptors involving account of both the alternative energy [source] and that of the entire PPS: one ratio comparing each of the maximum installed (or useful) powers (H_P); and, a second ratio comparing the extent of energy storage (H_E) of each:

$$H_P = \frac{P_{EL}}{P_{TOT}} \quad \text{and} \quad H_E = \frac{E_{EL}}{E_{TOT}} \qquad (1)$$

For a hybrid-electric solution, P_{EL} represents the maximum installed (or useful) electrical power, and P_{TOT} the total PPS installed power (motor, and thermal engine), E_{EL} the total stored electrical energy, and E_{TOT} the total stored energy of the entire PPS (electrical+kerosene).

The reader should be mindful about terminology the authors use when it concerns power: "installed" infers supplied power (what the battery or kerosene fuel delivers) corrected for energy conversion efficiency; and, "useful" is taken to be installed power additionally corrected for transmission and propulsive efficiencies. Furthermore, the convention adopted for H_E in this technical article alludes to the total energy available to the aircraft, i.e. the ratio of total electrical energy utilized for all phases of operation (whether block and/or diversion-contingency segments) normalized by the total energy comprising release fuel and electrical energy utilized for all phases of operation (whether block and/or diversion-contingency segments).

An equitable comparison calls for the possibility of examining a series of hybrid-electric aircraft PPS that deliver the same relative block fuel reduction or Energy Specific Air Range (ESAR) outcome. The ESAR figure-of-merit is fashioned to quantify distance travelled per unit of expended energy [2], viz.

$$ESAR = \frac{dR}{dE} = \frac{\eta (L/D)}{m\,g} \qquad (2)$$

The parameter dR/dE, which is pertinent for the evaluation of an overall block segment, represents the rate change in aircraft range for given change in expended system energy, η is the overall (combined exergetic) motive power system efficiency, L/D is the aircraft instantaneous lift-to-drag ratio, m is the aircraft instantaneous gross mass, and g is acceleration due to gravity.

Since the primary objective of this initial technical assessment study was to maximize the extent of emissions reduction over the entire payload-range working capacity. A special purpose top-level sizing algorithm was fashioned based upon the premise of meeting

multiple constraints. Using a suitably projected utilization spectrum for the aircraft, a generic multi-objective set could be fashioned in the manner presented by Fig. 1.

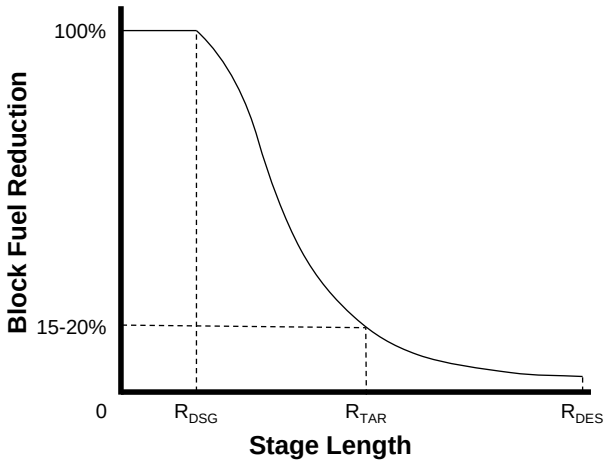

Fig. 1: Generic block fuel reduction multi-objectives for overall aircraft sizing

Here, R_{DSG} indicates the stage length corresponding to the Design Service Goal (DSG) of the aircraft, R_{DES} is the expected Max PAX range capability, and, R_{TAR} denotes the stage length wherein a significant block fuel reduction should be realized. As a general rule, R_{TAR} should aim to capture cumulatively 80-90% of all projected departures.

1.2 Aims of this Investigation

It is posited for commuter transportation, specifically, the 19-seater category, a revival of this long dormant market segment could occur by virtue of having ecologically benevolent attributes. Historically, 19-passenger turboprops have dominated the small commuter segment of aircraft with 40 seats or less; since the mid-1990s this particular market segment has seen lackluster interest from well-established operators. It is surmised market demand would increase substantially if an environmentally and community (noise) friendly 19-seat aircraft were to be introduced. The analogue drawn here is the spectacular success of 50-seat turbofans, which grew substantially from virtually zero in 1994 (including the emergence of 30-35 passenger jets to constitute a family concept). The introduction of hybrid-electric motive power technology into the 19-seater category is projected to have a similar impact, and, it is surmised that such vehicles would replace the current ageing turboprop fleet through operator trade-up in propulsion technology.

SAFRAN in-house pre-design work looking to perform an initial evaluation of hybrid-electric propulsion configurations for civil aircraft utilized expedient yet sufficiently detailed methods to conceive a 19 PAX fixed-wing commuter transport aircraft dubbed Propulsive ArChItecture For hYbrid Commuters, or, PACIFYC. By declaring a Beech 1900D as the reference, and mindful of retaining much of the original speed/altitude and payload-range working capacity operational performance attributes, perturbations from this seed aircraft were applied according to a given set of performance targets for advanced electrical machines, power electronics and secondary energy storage.

Representative motive power system configurations were evaluated in terms of design, integration, performance and operational characteristics, operating economics and potential for technological maturity by a target EIS of 2030. The final chosen candidates were then be compared to representative reference aircraft assuming identical mission roles, and, with engineering solutions that reflect state-of-the-art and advanced solutions featuring a conventional architectural approach.

To round-off the technical paper, 70-180 PAX hybrid-electric aircraft from previous investigations will then be compared and contrasted to this 19 PAX hybrid-electric concept with intent to understand the influence scale-effect has on sizing, overall aircraft performance and operating economics.

2 Aircraft Requirements, Objectives and Benchmarking Standards

Small-to-mid size commuter and regional aircraft design involves close attention to cost and weight sensitive factors that differ somewhat from larger passenger aircraft. These factors include: propulsion system bill-of-material and construction; weight and its relation to acquisition cost; design simplification for low tooling and production

costs; sensitivity to engine placement as it affects weight and balance, moment of inertia and drag; optimum wing loading and aspect ratio; a requirement for lower noise and emissions than for larger aircraft; and, freedom from ground support equipment.

2.1 Aircraft Requirements and Objectives

The Aircraft Top-Level Requirements (ATLeRs) that were deemed necessary for the success of PACIFYC study are defined below:

Tab. 1: Aircraft Top Level Requirements

Technology-Freeze Year / EIS	2025 / 2030
Design Range and Accommodation	700 nm, 19 PAX 102 kg per PAX 813 mm seat pitch
External Noise and Emission Targets Datum year 2000, interpolated SRIA 2030; from Ref. [1]	CO_2: -55% NO_x: -83% Noise: -53%
Take-off Field Length (TOFL) (MTOW, SL, ISA)	≤ 1200 m
Second Segment Climb	MTOW, DEN, ISA+20°C TOFL ≤ 1600 m
Landing Field Length (MLW, SL, ISA)	≤ 1100 m
Approach Speed (MLW, SL, ISA)	≤ 120 KCAS
AEO Service Ceiling and Typical Cruise	≥ FL250 ≥ M0.40
OEI Drift-down Altitude	≥ FL150
Miscellaneous	DSG 60000 cycles, 60000 FH 30 min. turn-around CS-25/FAR-25, Part 121 ops, EU-OPS 1.255

AEO – All-Engines Operational; FL – Flight Level; MLW – Maximum Landing Weight; MTOW – Maximum Take-Off Weight; SRIA – Strategic Research and Innovation Agenda

In the PACIFYC study, the multi-objective block fuel reduction problem as defined in Fig. 1 was set in the following manner:

- R_{DSG} = 150 nm (278 km)
- R_{TAR} = 430 nm (796 km), taken to be synonymous with capturing up to 85% of all life-cycle cumulative departures, at least 20% block fuel reduction
- R_{DES} = 700 nm (1296 km)

The mission profile consisted of taxi-out, take-off at sea level, en route climb until an initial cruise altitude of FL250. Cruise was performed at around M0.42, followed by a climb speed schedule mirrored descent, landing and taxi-in. All en route performance was assumed to occur under ISA ambient conditions. Reserves and contingency was based upon FAR 121 or equivalent EU-OPS 1.255 rules, namely, an IFR profile comprising 5% trip fuel (energy) contingency cruise, 30 mins hold at 1500 ft and 100 nm alternate.

2.2 Year 2000 and 2030 Reference Aircraft

The selection of reference aircraft was based upon the targeted application scenario and ATLeRs presented in Section 2.1. For purposes of gauging the relative merits of PACIFYC to that of interpolated SRIA 2030 targets, an appropriate transport aircraft reflecting an in-service year 2000 standard needed to be defined and analyzed. As this air transport task is, today, typically serviced by twin-engine commuter aircraft, a Beech 1900D equipped with Pratt and Whitney Canada PT6A-67D power plants was chosen as the State-of-the-Art Reference (SoAR) aircraft. Hence, a parametric model of the aircraft including the corresponding propulsion system was fashioned.

In order to appropriately capture the benefits of VJB concepts and to establish a suitable basis for consistent benchmarking, a reference aircraft reflecting the advanced technology level corresponding to an EIS 2030 application scenario was derived from the SoAR (designated as “REF2030”). Design range and payload were set in accordance with the ATLeRs given previously. In terms of mission performance, the REF2030 aircraft was predicted to deliver around 20% block fuel benefit compared the SoAR carrying a payload of 19 PAX at 102 kg per PAX.

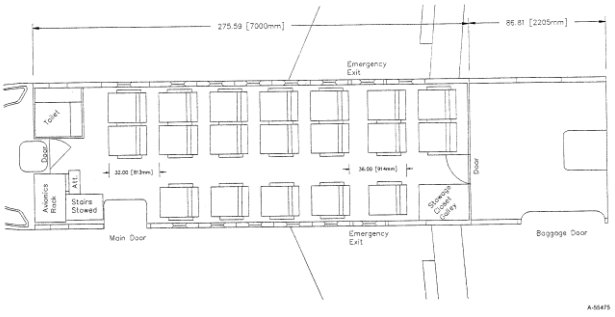

Fig. 2: Adopted cabin layout for REF2030 and PACIFYC; taken from Ref. [11]

Besides the adjustments to fuselage and cabin design taken from Ref. [11] in order to provide the required accommodation and future comfort standards (see Fig. 2 above for cabin layout), a set of aerodynamic, weights reduction, propulsion system and major systems related technologies appropriate for the targeted EIS was implemented compared to SoAR.

2.2.1 Airframe Aerodynamics and Structural Integration

An advanced flexible wing featuring an aspect ratio of 12.0 yielded a neutral lift-to-drag (L/D) outcome (at C_L = 0.55, M0.43, FL250) compared to the SoAR. This was attributable to the offset in wing related aerodynamic improvements due to the larger fuselage wetted area by way of REF2030 cross-section and cabin versus that of SoAR.

In keeping with assumptions made in Ref. [2] the structural design utilized advanced technologies such as omni-directional ply orientation of carbon fibers and advanced bonding techniques. This resulted in a reduction of 8% in structural weight relative to the SoAR.

2.2.2 Engines

The SoAR considered in this study is powered by two Pratt and Whitney Canada PT6A-67D engines. In order to perform investigative work and to quantify the gain from any VJB based hybridization, three distinct engines needed to be defined: two references and one bespoke engine for the VJB aircraft concepts.

The first reference architecture, the PT6A-67D as installed on the SoAR was used to calculate the current performance of the Beech 1900D. The second reference involved projecting this classical architecture to EIS 2030, taking into account potential improvements in the efficiency of turbo-components. For VJB aircraft concepts, it is more pertinent to evaluate performance in light of a suitably projected classical aircraft configuration with the same projected EIS. This enables an estimate of the gain (in terms of fuel consumption) of the hybrid-electric aircraft relative to a classical one taking into account the same technology level. In the following, "SoAR(E)" refers to the representation of the current PT6A-67D, "REF2030(E)" refers to the EIS 2030 projection of SoAR(E), and, "PACIFYC(E)" refers to a re-designed version of REF2030(E). See Section 3.2.3 for details about the PACIFYC(E).

SoAR(E)

The PT6A-67D has a distinct reversed-flow architecture as shown in Fig. 3. It is composed of an inlet, an axial compressor, a centrifugal compressor, a burner, a one stage high pressure turbine, a two stage power turbine, a gearbox, a high pressure shaft and a power shaft connected to a propeller.

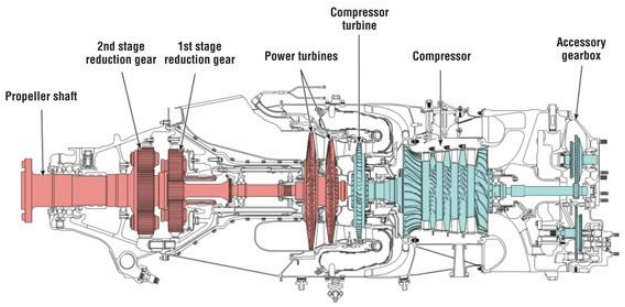

Fig. 3: PT6A architecture [12]

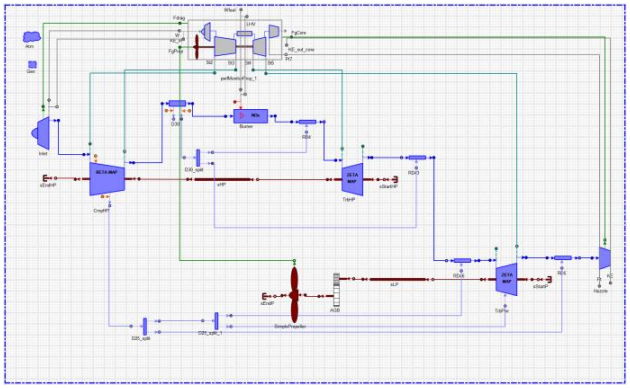

Fig. 4: PROOSIS™ of the SoAR(E)

The SoAR(E) architecture was modelled using the commercial engine performance simulation software PROOSIS™ [13]. In order to design or rescale an engine using PROOSIS™, geometrical and performance data are needed for one or more flight conditions and engine power levels. The values of certain parameters are imposed at these points leading to a representative model of the required engine. Different PT6A-67D [14-18] data sources from open literature were exploited in order to maximise information and precision for representing the engine. Assumptions were incorporated to obtain a robust simulation

model (see Fig. 4 above) and to subsequently fashion a suitable baseline for further modifications of the architecture. It is important to note that although the generated PROOSIS™ model is a good representation of a PT6A-67D turboprop it does not exactly reproduce the real engine performance. Some differences can be noticed but are considered acceptable for the scope of studies undertaken in this activity.

REF2030(E)

In view of the fact that REF2030(E) has the same architecture as SoAR(E), it was assumed the components type and order, the cooling scheme and the design hypothesis made for SoAR(E) remain valid. The important modifications for a REF2030(E) relate to the state-of-the-art of the components, the temperatures and some other variations.

The following modifications and critical assumptions constituted the projection exercise:

- Evolutionary pathway based upon analogues taken from similar engines, e.g. High Pressure Turbine (HPT) inlet temperature evolution over a 30 year timeframe for turboshaft and turboprop engines in the same power range
- The same propeller is used for all types of propulsions systems. The design of the propeller was neither updated nor adapted and does not invoke any improvement for an EIS of 2030
- The redesign considered no change in power and thrust specifications between SoAR(E) and REF2030(E)

Improvement in efficiencies of the turbo-components and the thermodynamic cycle variables, namely, HPT inlet temperature and the Overall Pressure Ratio (OPR) are the main sources of improvement in fuel consumption. The assumptions are itemized as:

- +40 K in HPT inlet temperature at design Maximum Take-Off (MTO)
- +26.5% in OPR (from 9.5 to 12.0)
- Improved turbo-component efficiencies, see Tab. 2 for details

The Thrust Specific Fuel Consumption (TSFC) was predicted to be -20.4% at typical cruise and -22.6% at take-off conditions. The Power Specific Fuel Consumption (PSFC) was predicted to decrease by 21.4% at typical cruise and 23.6% at take-off.

Tab. 2: Turbo-component efficiencies during cruise of REF2030(E); MTO as design point

	HPC	HPT	LPT
Polytropic Efficiencies	0.871	0.834	0.864
Incremental Delta from SoAR(E)	+0.025	+0.053	+0.091

HPC – High-Pressure Compressor
LPT – Low-Pressure Turbine

It should be noted that all engine designs discussed in this paper were bounded by the following constraints:

- Engine operability and transient phases were not considered. A check of the surge margins stack up was made without any further optimization
- The Nozzle Pressure Ratio was kept at a value of 1.05-1.10. This influences the mass flow and the nozzle area which are checked and validated to avoid integration issues

2.2.3 Major Systems

Major systems encompasses the Environmental Control System (ECS), the Anti-Ice System (AIS), Landing Gear (LG) and the Flight Control System (FCS).

ECS pressurization and air-conditioning for the flight deck, cabin and cargo hold are provided by bleed air from the engines. The system is operated through two air cycle packs located in the wing-fuselage fairing. Conditioned air is supplied from the air cycle packs by separate lines to the flight deck and cabin.

The AIS provides protection for the wing and horizontal stabilizer leading edges, windshields, engine inlets and air-data sensors. Anti-icing of wing and stabilizer leading edges is accomplished by means of a bleed-air system via piccolos combined with electrical heaters – no de-icing boots are used. The vehicle employs electrical anti-icing for nacelle intake lips.

The LG is a tricycle type arrangement consisting of two main gear assemblies mounted

at the root of each wing, and a nose gear mounted on the forward fuselage beneath the flight deck. Extension and retraction is facilitated by electro-hydrostatic actuators and is electrically controlled.

The FCS comprises ailerons, elevator and rudder, flight and ground spoilers, flaps and variable incidence tailplane. Control is segmented into primary and secondary systems. The primary control surfaces are mechanically actuated by conventional floor mounted control columns and adjustable rudder pedals complemented by cables, pulleys, bell-cranks and rods. The elevator and aileron control paths are redundant and the control path is duplicated where required. A gust lock system is also provided and is operable from the flight deck. Trim tabs on all surfaces are controlled by redundant electromechanical actuators.

3 Multi-disciplinary Design and Analysis of Hybrid-Electric Motive Power Systems

A coherent, standardized and robust set-up in conjunction with adherence to strict procedural control was needed to ensure successful multi-disciplinary interfacing, sizing and optimization. Details about these aspects including down-selection are given below.

3.1 Down-selection Framework, Concept Cloud and Results

The down selection procedure aims to qualitatively assess the attributes of different candidates in comparison to one architecture that is chosen as the reference (tentatively, from what is considered to be the designer's choice). In order to compare "performance", several criteria of merit were chosen. Those criteria were organized and classified into four main groups, and, "casting" during the down selection session was done by different specialists able to qualitatively assess the different architectures according to each criteria.

3.1.1 Down-selection Framework

During the down-selection exercise concept clouds comprising four candidate designs for VJB based architectures were qualitatively rated against a total of 15 sub-categories which were grouped into four main criteria with technical, operational and certification related foci:

- Propulsion
- Weight and Integration
- Certifiability and Development
- Operations

Each main criterion included a set of three-to-four specific sub-categories. The weightings of the main criteria and sub-categories were tailored to reflect the emphasis placed upon fuel burn and operating cost reduction. Thus, one of the main criteria having a major impact on fuel burn, "Propulsion", was assigned a weighting of 0.337, whereas, the "Weight and Integration" criterion deemed as one exhibiting a mixture of fuel burn impact together with operating cost influence was weighted with 0.260. The two remaining criteria, "Certifiability and Development" and "Operations", were weighted with 0.230 and 0.173 respectively. These values are quoted to three decimal places because it reflects an average given by 16 specialists. The final array of scoring was attained by evaluation of each individual concept against what was intuitively deemed the best design candidate from within a pool of four.

In addition, technical maturity was assessed by evaluating each concept with respect to the likelihood of success and the effort to bring the technology to target Technology Readiness Level (TRL) 6 by technology freeze in year 2025. Following the procedure described by Ref. [19,20], robustness of the concept rating was gauged by systematically varying the criteria weighting in each main category. This was achieved by means of artificial amplification in such a way one category was rated with 0.40 and the remaining weightings were equally distributed amongst the other main criteria.

3.1.2 Concept Cloud of Architectures

Four VJB propulsive architectures were identified for purposes of down-selection in this study:

1. **ARCH 1** – Electrical Booster
2. **ARCH 2** – Hybrid Turbo-electric

3. **ARCH 3** – Dual Propulsion with Exchangeable Battery
4. **ARCH 4** – Electrical Booster with Exchangeable Battery Pack

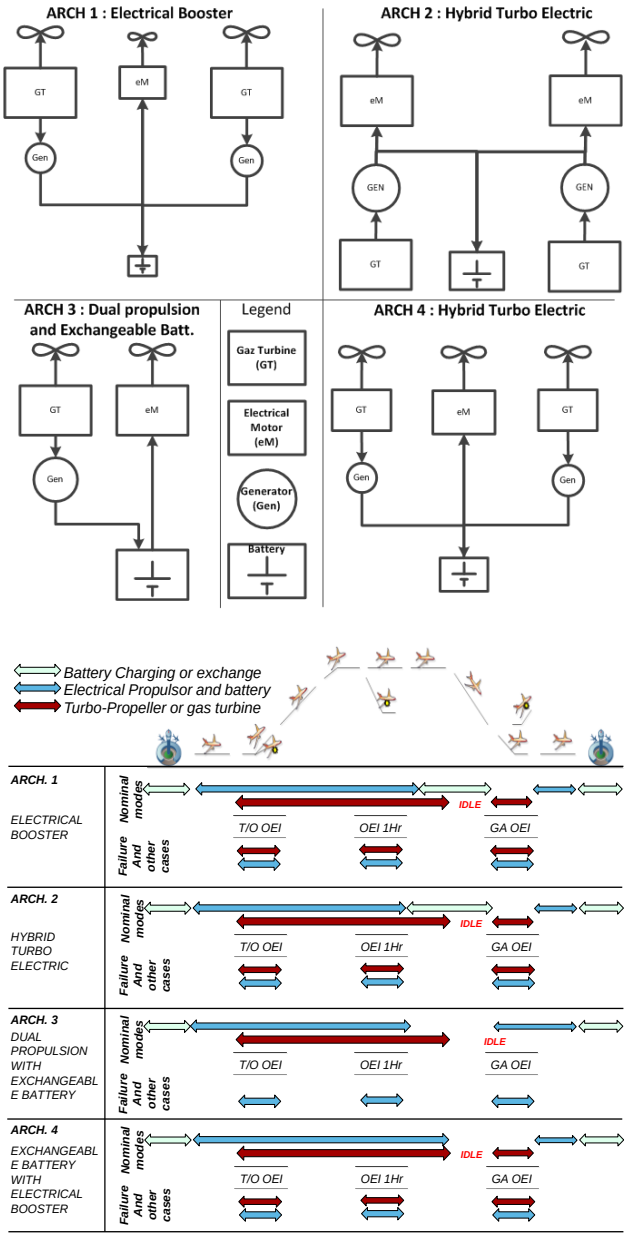

Fig. 5: Architecture candidates and corresponding operational modes considered in the PACIFYC down-selection

At this pre-design level of the study, only a macroscopic definition of each architecture was made available. Any degrees-of-freedom related to operational modes and aircraft morphology were subject to choice and further refinement *a posteriori* to the down-selection exercise. A corresponding set of operational modes according to each architecture type was also stipulated from the outset. See Fig. 5 for schema corresponding to each architectural candidate.

The main objective of ARCH 1 is to relax the design of the thermal engine in terms of performance. Specifically, the engine should be designed for only one rating, namely, Maximum Cruise, and the available thrust available at T/O is considered to be a fall-out. To compensate the loss of power at T/O (and on others specific phases like climb and OEI) an electrical propulsion device is added but batteries are used as the main power source. Also, this electrical propulsion group could be used in descent (wind-milling) to recover energy.

ARCH 2 is based on the same principle as ARCH 1 but the propulsive configuration is in serial: two thermal engines connected to two electrical generators that power two electrical motors. A battery is also used to smooth any power peaks of the gas turbines.

ARCH 3 introduces the concept of full exchangeable battery packs at the end of the flight. In this case the battery is used as an energy source. To optimize the number of parts in the architecture, only one turbo-prop and one electrical motor with a propeller is used.

ARCH 4 is a mix between the concept of ARCH 1 and the exchangeable battery concept: the thermal engine(s) are optimized for one specific rating and the batteries also deliver supplementary energy during the mission.

3.1.3 Down-selection Results

As a result of the down-selection process (see Fig. 6 for outcomes), ARCH 1 and ARCH 4 were identified as the most promising candidates. These were also assessed to be concepts with the highest potential to meet the target technical maturity level compared to the other rated alternatives. In order to adequately address system redundancy stipulated by transport category certification, the aircraft morphology chosen for ARCH 1 and ARCH 4 comprises two on-wing podded turbo-props.

ARCH 1 scored the highest when integration is given the highest relevance. ARCH 4 has a lower standard deviation in the scoring compared to ARCH 1, hence providing a more robust solution but exhibits more risk. A targeted aircraft performance improvement of

20% or more block fuel reduction is achievable with an "Electrical Booster + Exchangeable Batteries" concept, and thus, it has a higher risk value compared to ARCH 1 due to the influence of battery performance in the technology outlook. Irrespective of this, ARCH 4 out-performs every other concept with regards to propulsive performance including emissions and aero-propulsive efficiency (dark green bars in the chart shown in Fig. 6).

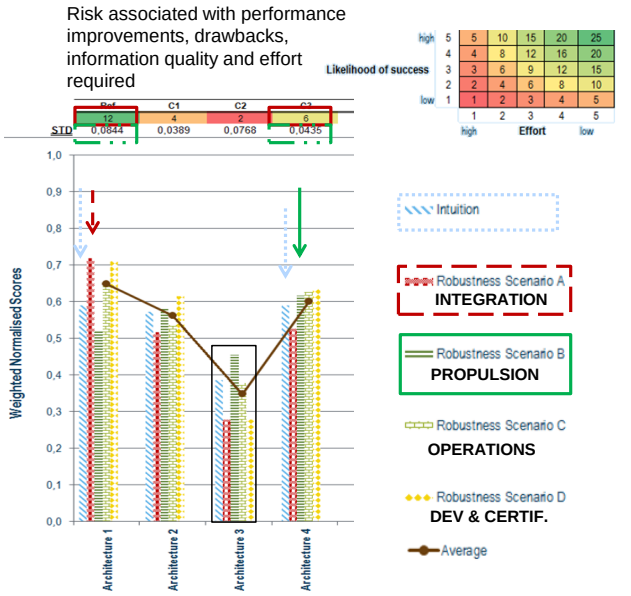

Fig. 6: Results of robustness analysis of hybrid-electric propulsion architectures

ARCH 3 did show some merit, however, due to forecasted levels of battery energy density, it obtained the lowest score regarding integration, development, certifiability and operational criteria. Such an outcome should not preclude revisiting this solution in future investigations provided higher battery energy densities can be realized.

3.2 Multi-disciplinary Constituents

This section describes the components that constitute advanced VJB motive power systems. Performance targets and efficiencies are presented mindful of EIS 2030.

3.2.1 Electrical Power Chain and Batteries

Electrical architectures indicative of ARCH 1 and ARCH 4 need to ensure reliable and steady power supply from either the thermal engine generator or electrical storage device. Fig. 7 displays a simplified schematic of the necessary architectural interfaces and offers a general description of important facets.

Electro-mechanical conversion is to be performed using an Alternating Current (AC) voltage machine, whereas, electrical storage utilizes Direct Current (DC). As no AC power sources are to be used in parallel with another one, the main power transfer will be performed via a DC link. To this end, each electrical machine has a dedicated AC/DC converter. Battery current regulation needs are covered using current-controlled AC/DC converters. In this fashion, no additional DC/DC converters are to be used, thus allowing for weight reduction and ameliorating failure mode cases.

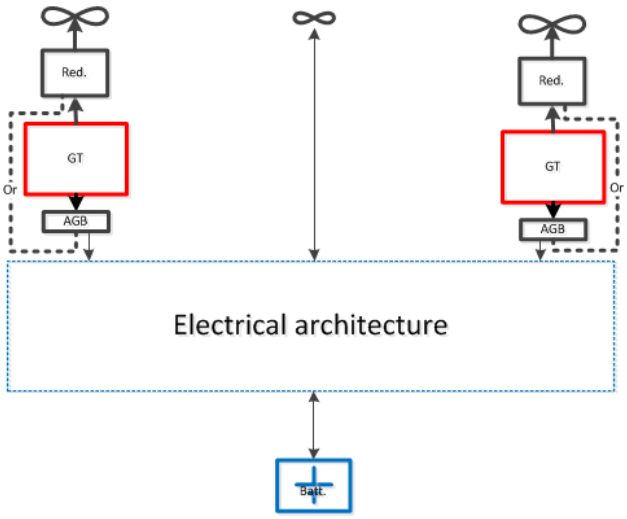

Fig. 7: Electrical architecture interfaces compatible for ARCH 1 and ARCH 4

3.2.2 Properties and Performance Targets

Tab. 3 gives an overview of properties as well as performance targets for electrical component options. A discussion motivating the targets given for electrical machines, power electronics and thermal management is also provided.

Propulsive Element

Permanent magnet rotors have the highest power-to-weight ratio and are expected to achieve 9.0 kW/kg by year-2030 [22]. This approach does impose the use of an inverter to control speed. This inverter is to include the latest Si-C components, thereby limiting internal loss. These kinds of converters may reach a high level of efficiency, however, since it will need to be used in a reversible fashion,

e.g. in an emergency case, and are required to control propeller speed this would tend to reduce its efficiency to around 95%. The power density linked to this element is considered to reach 10.0 kW/kg. As a result the global propulsive system is projected to have 4.8 kW/kg with a corresponding 90% in overall efficiency.

Tab. 3: Properties and electrical component performance targets

Property or Component	Sizing Param.	Effici-ency
Fuel Energy Density (kWh/kg)	11.8	N/A
Battery Energy Density (Wh/kg)	500*	
Battery Power Density (W/kg)	1000*	
Battery Volumetric Density (Wh/L)	500**	
Battery Charger Power Den. (kW/kg)	15.0	97%
Motor Power Density (kW/kg)	9.0	95%
Generator Power Density (kW/kg)	5.0	90%
Power Electronics Power Den.(kW/kg)	10.0	95%
Bus Voltage	540 VDC	N/A
Aluminium Transmission (kg/m)	5.8***	~100%
Thermal System Penalty (kW/kg)	1.5	N/A

* System-level requirement
** Based on Ref. [3]
*** Based on Ref. [21]

Electrical Energy Generation

In order to allow use of generators for non-propulsive loads, a three-stage generator has been chosen since it can easily manage failure modes and allows for RMS voltage control by way of digital excitation. This kind of generator is expected to exhibit 90% efficiency at 5.0 kW/kg by EIS 2030. It supplies a Thyristor Rectifier Unit that controls the output current. Thyristor Si-C technology is postulated to be sufficiently mature by year-2030 with an expected efficiency of 97% and corresponding power density of 15.0 kW/kg. Overall electrical energy generation performance is targeted to be 10.0 kW/kg with 87% efficiency. If required design power coincides with the order of magnitude of the aircraft generator (to provide electrical power to the aircraft systems), these generators have a possibility of being shared.

Electrical Storage

Electrical storage includes the electro-chemical cell, balancing system and packaging. These aspects are taken into account because no safe use of chemical cells can be realized. Two characteristics are used for storage sizing: (1) energy to be stored; and, (2) power to be supplied. Li-S battery technology has been selected due to the potential for high energy and power mass densities (500 Wh/kg and 1000 W/kg respectively) at system-level. At this point in time, this technology is not sufficiently mature for use on aircraft, however, there is scope for the first generation of Li-S to be used by 2030 [23].

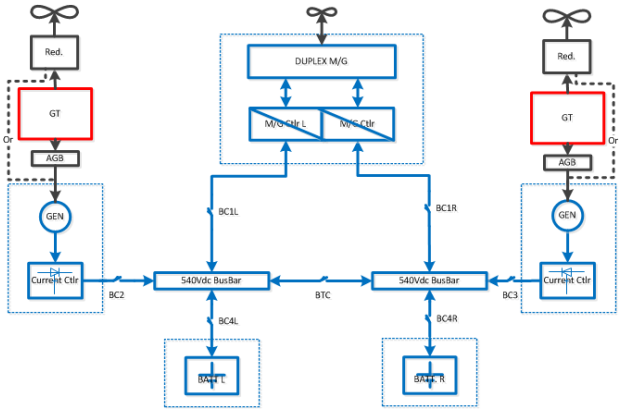

Fig. 8: Final electrical system architecture incorporating fail-safe features

Electrical System Robustness

When surveying the overall electrical architecture the least reliable element is the inverter, which is tasked with supplying the propeller. This aspect needs to be compensated through redundancy. Moreover, as its power is high, use of two inverters supplying a hexa-stator machine may increase significantly system availability without invoking a penalizing mass impact. In view of this consideration the final electrical system architecture adopted for the design candidates is depicted in Fig. 8 above.

Thermal Management

In view of the electrical power channel facilitating a significant amount of power,

thermal losses need to be managed thoughtfully, and, such a consideration is linked to electrical power conversion, high power density and efficiency. As the storage power density is taken to be rather low, the need for a dedicated heat exchanger does not exist. In addition, since the batteries are stored in a non-severe environment (not close to the thermal engine) problems associated with overheating are not envisaged. Contemporary controlled rectifiers have a sufficient efficiency to be cooled using forced air devices. In contrast, electrical generators need to be cooled, and a typical approach involves an oil cooling system. As such, this will have a mass impact on global system.

Electrically driven propellers, including power electronics and electrical motor, are the most critical elements since they operate at the highest power level. It may be installed close to, or, within the aircraft air flow, and, even if an optimized heat exchanger is incorporated this will impose a significant mass impact. To take into account the penalty of a global cooling system, in-house knowledge assessed the penalty in mass to be 1.5 kg per extracted thermal kilo-Watt. Moreover, additional heat exchangers might be required to ensure improved global system efficiency. The potential additional drag expected by this type of device may be at least compensated partially (even completely) with an adequate integration that fully exploits the Meredith effect [24], i.e. a radiator that provides adequate cooling flow and reduces the drag associated with the installation.

3.2.3 Engine Design Specific to Hybrid-Electric Applications

In general, designing an engine is a complex process taking into account different constraints. The final design cycle and performance are the results of the best compromise found between constraints of operability, integration, aging, cost and fuel consumption for a given aircraft and missions. In such a process, some specific operating points are critical even though they are operated for a very short period of time compared to the whole mission. Take-off represents one of the critical and constraining design conditions. It lasts for a short amount of time but it imposes limits on the temperatures and engine size for the rest of the operations. In fact, engines typically reach maximum allowed temperatures at take-off for maximum power, and any thrust demand including both safe operation and failure modes need to be taken into account within the design.

The take-off phase has very little impact on total fuel consumption; nevertheless, due to stringent operating conditions, the engine needs to be oversized for safe operation. Therefore, longer phases such as cruise are impacted by this oversizing and their performance is a consequence of it. Removing some design constraints to optimize the engine for cruise and assisting the engine during the critical phases is investigated in this paper.

The PACIFYC(E) version for VJB application needs to be optimized for cruise performance, and as such should be compared to REF2030(E). The performance of the PACIFYC(E) is calculated at design and off-design points that are the most constraining in terms of power. These calculations determined:

- The extent to which electrical assistance is advantageous at high power operating points such as take-off
- The gain in performance at some mission points both at engine-level and aircraft-level

With regards to iso-shaft power, the new cycle was designed at a higher cruise OPR (13.8) and a higher T41 (1350 K). The other parameters, such as the high pressure compressor rotational speed, were adapted to these modifications accordingly. The implication of this was to add approximately 0.5-1.0 percentage points of polytrophic efficiency to the compressor and turbines.

The impact on critical mission points should also be quantified to estimate the required amount of electrical power assistance deemed to be of high importance in the context of the global energy balance. Assuming EIS 2030 limitations, reducing the core size of the engine at cruise will limit the take-off available power. The thermal engine alone cannot provide this power as the mechanical speed of would exceed the limitation of 39000 RPM and the HPT inlet temperature would surpass an upper

limit of 1380 K. Therefore, the maximum power that could be delivered by this new engine at take-off, the most critical point of the mission, is assessed by running the model to its maximum limits.

At maximum T41 Take-off, the thermal engine power was found to be lacking 14.1% of the total required power and this difference has to be provided by the electrical system. This difference in power was imposed upon the design specifications of electrical production, conduction, conversion and corresponding storage systems.

Improved turbo-component efficiencies associated with the specially designed PACIFYC(E) is shown in Tab. 4. The comparison is made assuming SoAR(E) as well as REF2030(E), and as it can be readily observed a significant improvement in turbo-component efficiencies can be gained when attempting to customize the thermal engine for hybrid-electric applications.

Tab. 4: Turbo-component efficiencies during cruise of PACIFYC(E); cruise as design point

	HPC	HPT	LPT
Polytropic Efficiencies	0.880	0.860	0.870
Incremental Delta from SoAR(E)	+0.034	+0.079	+0.096
Incremental Delta from REF2030(E)	+0.009	+0.026	+0.006

The performance outcome showed a 5.9% improvement in TSFC over and above the REF2030(E) according to this redesign assumption. In addition, the PSFC during cruise was predicted to be -4.3%.

3.3 Operating Economics Analysis

In an effort to foster more realistic product development considerations related to aircraft sizing this initial technical assessment activity coupled Cash Operating Cost (COC) into the scheme. Cost of Ownership (which includes depreciation, interest and insurance costs) was intentionally neglected owing to considerable uncertainties in establishing the value of such advanced engineered products [2]. The methodology and pertinent array of critical assumptions was based upon those published in Ref. [2].

The COC sums up expenditures for fuel, crew, maintenance, airport and en route charges. The principal crew cost model is based on the Association of European Airlines (AEA) methodology where crew hourly rates are a function of Maximum Take-Off Weight (MTOW) and number of PAX [25,26]. It was subsequently tuned according to scaled data found in Ref. [27]. An explicit model addressing additional costs associated with handling battery modules during turn-around was not devised. For purposes of this study, the handling of battery modules was taken to be analogous to that of cargo containers. The cargo container handling cost constituent model is expressed as a function of MTOW [28]; and since VJB based aircraft concepts have a tendency of generating higher MTOW candidates compared to any baseline or seed aircraft, it was argued such an approach would serve as a suitable proxy for capturing incremental costs associated with battery module handling.

The Direct Maintenance Cost (DMC) covers labor and material cost associated with airframe and engine. Operational dependencies, such as flight cycle and flight time are also considered. The airframe DMC are calculated with an analogous costing method given in [29] and the engine DMC are determined using parametric cost functions in [30] and tuned in accordance with information found in Ref. [31,32]. Appropriate capture of airframe and propulsion DMC related to VJB based designs involved the following modifications (itemized according to Air Transport Association, ATA, chapter convention):

- ATA 32 Landing Gear – variation in certified design weights
- ATA 53 Fuselage – variation in certified design weights
- ATA 54 Nacelles and Pylons – housing of additional motive power components based upon electrical machines
- ATA 71 Power Plant – additional power transmission bill-of-material items

All analysis results reflect a year-2012 standard and the working currency was assumed to be US dollars (USD). Also, the results reflect a "Year-1" study neglecting aging or deterioration effects. Kerosene fuel price was nominally assumed to be USD3.30 per USG [33], and with intent to gauge sensitivities, a lower value of USD2.00 per USG and an upper limit of USD6.00 per USG were declared. The global average electrical energy price weighted according to total flight operations in 2012 accounts for USD0.1109 per kWh [34]. By using this min-nominal-max bandwidth of values, it provided a means of treating the operating economics analysis in a non-deterministic manner.

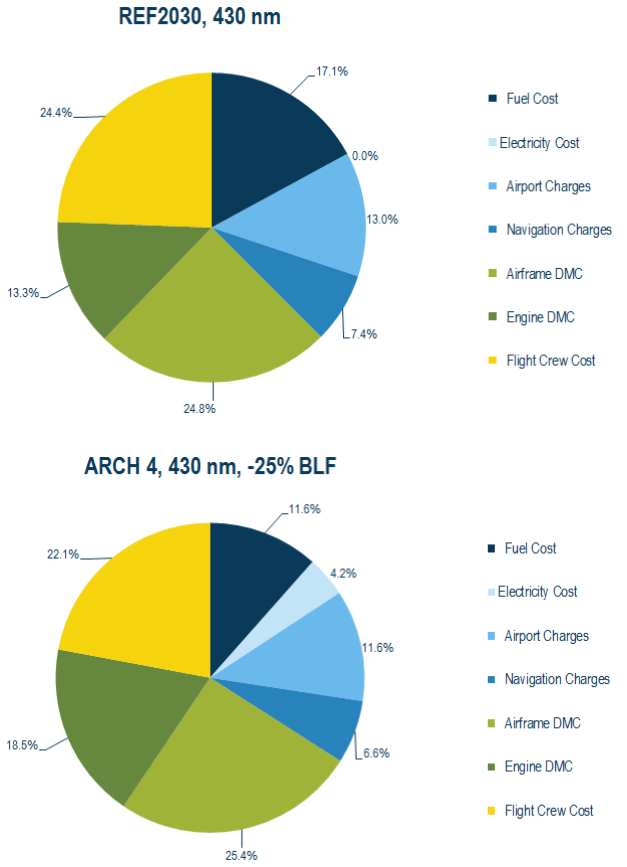

Fig. 9: Generic block fuel reduction multi-objectives for overall aircraft sizing

Figure 9 presents cost component breakdowns for the REF2030 and VJB based motive power design option called ARCH 4 covering 430 nm. See Section 4 for details about the morphological and integration strategies associated with the ARCH 4 concept together with the ARCH 1 alternative.

Prior to proceeding with the complete analysis, it was noted from Ref. [2] cost constituents like landing fees and navigation charges could unfairly distort costs because of an explicit functional relationship with design weights. Since VJB based aircraft tend to be heavier in weight it was reasoned these cost components should be held fixed, i.e. equal to the REF2030 projected turboprop only aircraft, in recognition of the significant emissions reduction potential of aircraft employing VJB motive power systems versus those that do not. In the results to follow, this adjustment been incorporated.

3.4 Aircraft Design Axioms and Heuristics

For sake of simplification, all component efficiencies were considered to be invariant with operating time (changes in loading behavior). Except for structural systems, all specific weights were taken to be independent of scale (sizing variations). All aircraft variations away from the REF2030 aircraft reflect a common all-axes dimensional wing scaling and constant wing loading, thereby retaining the same en route buffet onset characteristics. The empennage was primarily scaled with wing geometric variation according to a constant volume coefficient approach; however, where appropriate, sizing did take stock of minimum control speed vertical tail control power requirements.

Identical application of operational rules, payload, stage length, and where possible, flight technique were employed to that of the REF2030 aircraft attributes presented in this treatise. The integrated performance analysis employed here utilized simplified flight mechanical and performance methods in order to map required power and energy profiles during the integrated takeoff, three-phase climb, cruise and descent subject to transversality conditions, and, landing phases.

The fuselage geometry was initially kept fixed for all variations away from the REF2030 aircraft, and as a result, it was conceivable some analyzed candidates would violate minimum volume allocations for cargo and/or the alternative energy source. Displaced volume

due to presence of batteries and associated thermal management system was assumed using a linear volumetric specific energy model computed from the product of battery energy density and 1000 kg/m^3 as given in Tab. 3. Any changes to the fuselage Outer Mould Lines OMLs) due to increased volumetric to house batteries were implemented including account of incremental wetted area and fuselage weight. Finally, apart from the application of simplified geometric rules, such as, the centre-of-gravity being placed according to a constant non-dimensional longitudinal fuselage location of the wing Mean Aerodynamic Chord, aircraft balance and any associated impact to trim have been neglected.

A pool of aircraft morphological candidates able to facilitate the integration of a tri-prop propulsion system is presented in Fig. 10. Assuming two of the propellers shall be arranged as on-wing podded installations, possibilities include a nose-mounted tractor (denoted as "A"), cruciform empennage-mounted tractor (similar to the Britten-Norman Trislander, denoted as "B"), "H-tail" empennage with pusher (denoted as "C"), and the "V-tail" empennage with pusher (denoted as "D"). When choosing the most appropriate morphology, issues related to propeller efficiency and blockage, avoidance of channel flow (localized super-velocity formation), simplification of bill-of-material, nose-wheel collapse and tail-scrape geometric limitations, blade-off ramifications, detrimental colocation of essential systems, motor cooling, aircraft balance, propensity to excessively perturb OMLs, clearances including that of ground and avoidance of sonic fatigue on localized structure, as well as aesthetic appeal, were reviewed. After carefully weighing the relative merits (or otherwise) of each morphological option, the decision was made for ARCH 1 to adopt the H-tail empennage with pusher, and, ARCH 4 to employ the V-tail empennage with pusher.

3.5 Sub-space Coupling and Analysis Flow

Figure 11 describes the sizing loop of ARCH 1. The main objective was to align the need in terms of electrical power to the need in energy provided by the battery. By decreasing the reference thrust of the thermal engines, correspondingly, required electrical power and energy tends to increase. Due to the fact that the need in energy grows faster than the required electrical power, the best compromise in the design scenario can be reached when all the usable battery energy is consumed.

The second concept, ARCH 4, also utilises a third propeller driven by an electrical motor with electrical energy supplied by a battery. The objective in this instance is to achieve at least 20% fuel burn reduction for the 430 nm mission. The consequence on the design is the overriding reliance on batteries, which are to be replaced at the end of the mission. The baseline to this concept used the results of ARCH 1 with its already optimized engines.

The electrical systems design of ARCH 4 focused on the 430 nm mission. The necessary quantity of battery to reach the 20% fuel burn reduction goal is inserted in the aircraft along with a de-rating of the thermal engine (see Fig. 12). The off-design missions were realized by establishing an adequate energy repartition

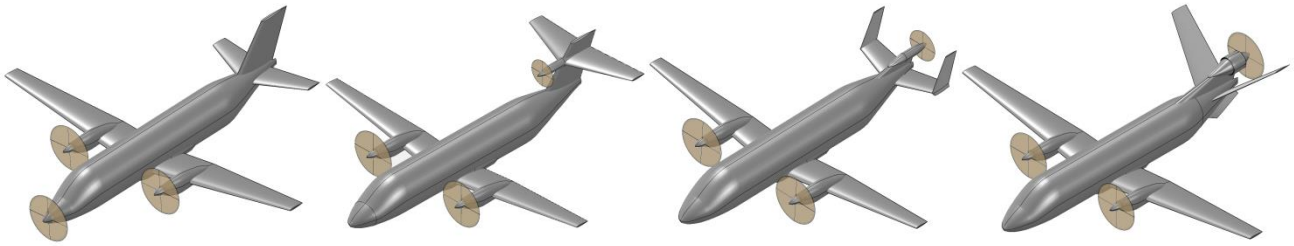

A **B** **C** **D**

Fig. 10: Aircraft morphological candidates that were considered (A) nose-mounted tractor, (B) cruciform empennage-mounted tractor, (C) "H-tail" empennage with pusher and (D) "V-tail" empennage with pusher

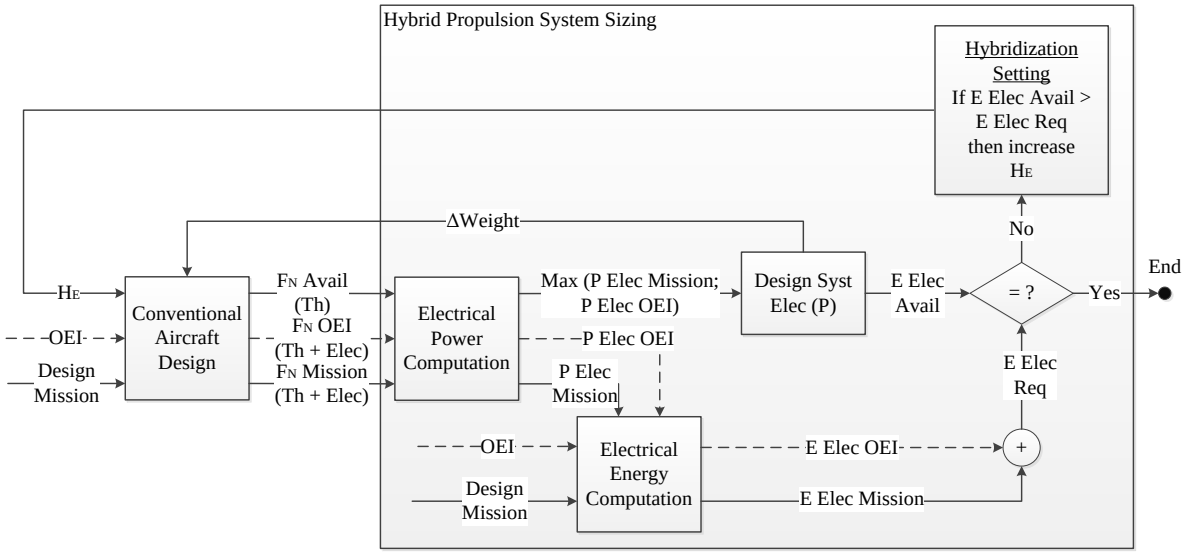

Fig. 11: ARCH 1 sizing loop

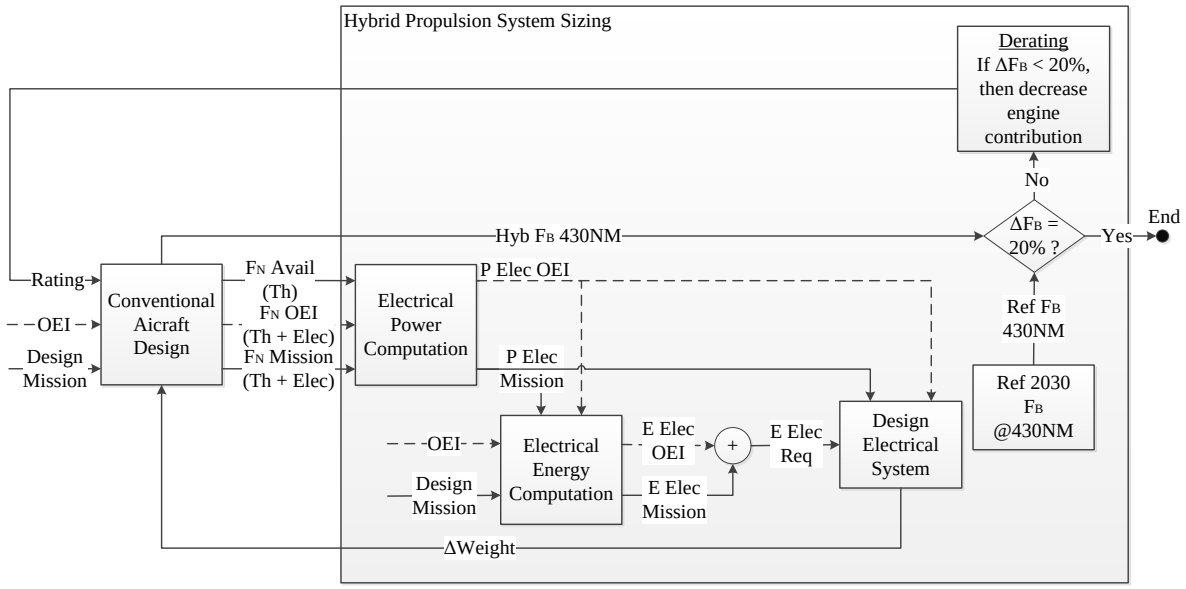

Fig. 12: ARCH 4 sizing loop for the 430 nm mission

between the fuel and the batteries. In order to complete the 700 nm mission, part of the batteries were removed from the hybrid vehicle to make room for additional fuel, thereby invoking a useful energy load trade for sake of completing the maximum design. Regarding the 150 nm mission, the engine was systematically "flexed" (reduced power) until the electrical system capabilities were fully exploited.

To round off, the 19 PAX hybrid-electric concepts were sized based upon a two-pronged set of objective functions: (1) relative block fuel reduction; and, (2) operating economics. The objective function of operating economics serves as a counterpoint to the relative block fuel result, thus ensuring a more pragmatic selection is made when it concerns electrical-to-kerosene energy storage ratio, power-split between propulsive device types and associated relative utilization (with respect to time) afforded by the motive power device associated with each energy source.

All computational work was performed using the PACE suite of tools [35]. These included Pacelab APD™ for overall aircraft conceptual design sizing and integrated performance analysis, and, Pacelab SysArc™ used to perform multi-layered integrated systems sizing. All OMLs visualization was conducted using the OpenVSP open source

parametric geometry toolkit developed by NASA [36].

4 PACIFYC General Design Description, Evaluation and Benchmarking

The ARCH 1 and ARCH 4 motive power system configurations were evaluated in terms of design, performance and operational characteristics. These solutions were then compared against representative reference aircraft (SoAR and REF2030) assuming identical mission roles.

4.1 Overall Design Sizing Outcomes

A synopsis of important aircraft characteristics for the SoAR, the REF2030 and the selected ARCH 1 and ARCH 4 designs is given in Tab. 5. It is highlighted all relative values quoted in the data table and discussion text thereafter adhere to the convention of fractional change. The analytical basis of fractional change operates with the underlying premise that the designer/analyst begins with a seed condition or aircraft. By considering an increment in variable x as dx or Δx, a fractional change to a new value, x_1, small or otherwise, from a seed parameter x_o is defined as

$$\triangleleft x = \frac{\Delta x}{x_o} = \frac{x_1 - x_o}{x_o} = \frac{x_1}{x_o} - 1 \qquad (3)$$

Notional differences in sizing when comparing the SoAR aircraft (not optimized for 700 nm maximum design range assuming 102 kg/PAX), the REF2030 and the proposed ARCH 1 and ARCH 4 is shown in Fig. 13 overleaf. The SoAR block fuel for a 430 nm stage length was established to be +34% in

Tab. 5: Comparative synopsis of important aircraft characteristics

		SoAR	REF2030	ARCH 1*	ARCH 4*
Design Max Range	[nm]	680 (200 lb/PAX)	700 (102 kg/PAX)		
Accommodation	[PAX]	19			
MTOW	[kg]	7766	7880	8490	11020
Operational Weight Empty (OWE)	[kg]	4847	4962	5603	6331
OWE / MTOW	[-]	0.624	0.630	0.660	0.575
MLW	[kg]	7605	7722	8320	10800
Ref. Area, Geometric (S_W)	[m^2]	29.08	29.50	31.78	41.26
Wing Aspect Ratio, Geometric	[-]	10.42	12.00		
Wing Span	[m]	17.4	18.8	19.5	22.3
Fuselage Length	[m]	17.2	17.6		
Wing Loading (MTOW / S_W)	[kg/m^2]	267			
Total Max. Static Power (ISA, SLS)	[kW]	1908	2025	295 motor 1935 total	1105 motor 2745 total
Power-to-Weight (SLS, MTOW)	[kW/kg]	0.246	0.257	0.228	0.249
Typical LRC	[-]	M0.38	M0.42	M0.40	M0.42
◁L/D (Typ. CRZ, ISA)	[-]	datum @FL230	+7.9% @FL250	+6.7% @FL250	+11.2% @FL250
Payload, Max PAX, Typ. CRZ, ISA	[kg]	1938			
◁Block Fuel, 150 nm (R_{DSG})	[-]	datum	-16.1%	-26.1%	-48.7%
		+19.4%	datum	-11.5%	-38.8%
◁COC, 150 nm (R_{DSG})	[-]	+1.2%	datum	+3.0%	+8.0%
◁Block Fuel, 430 nm (R_{TAR})	[-]	datum	-25.5%	-33.5%	-43.9%
		+34.3%	datum	-10.7%	-24.7%
◁Block ESAR, 430 nm (R_{TAR})	[-]	-25.6%	datum	+11.9%	+11.6%
◁COC, 430 nm (R_{TAR})	[-]	+4.6%	datum	-2.1%	+11.5%
◁Block Fuel, 700 nm (R_{DES})	[-]	N/A	datum	-3.0%	-10.3%
◁COC, 700 nm (R_{DES})	[-]	N/A	datum	-0.6%	+13.6%

* Electrically powered ground maneuvering

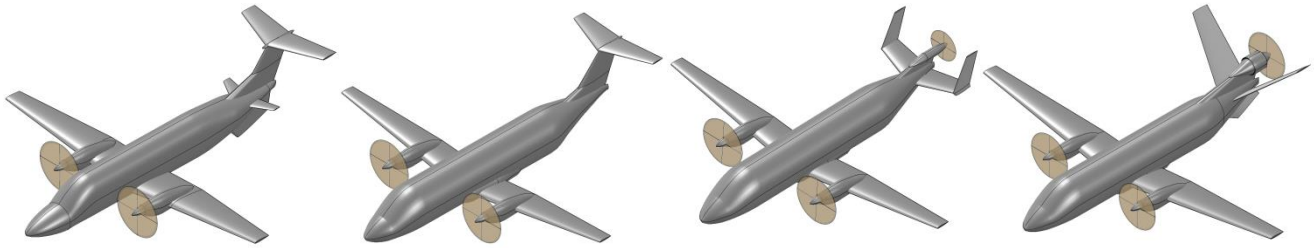

A **B** **C** **D**

Fig. 13: Notional contrast in sizing between the (A) SoAR [Beech 1900D], (B) REF2030, (C) ARCH 1 and (D) ARCH 4

relation to the REF2030. A significant increase in MTOW and wing area is associated with ARCH 4 compared to the REF2030; in fact, the values are both +40%. Although it might appear discouraging, the reader is reminded that the payload-range working capacities of the aircraft are identical.

Evaluation of ARCH 1 for the design and off-design missions show even though the fuel burn goals of this study are not reached the VJB aircraft candidate has very promising results in terms of block energy efficiency (see ESAR in Tab. 5 and Fig. 14). A non-negligible advantage of this solution is the operational flexibility offered by an in-flight battery recharge capability. Indeed, a battery energy neutral-expenditure scenario is conceivable by coupling the design with flight profile adjustments. A flight technique is suggested here to land with an equal State-of-Charge to that of the beginning of the mission. As can be observed in Tab. 5 this customized flight technique tends to slow down the cruise speed, increasing flight time by 4-6 mins.

It is highlighted that a variety of scenarios are possible with ARCH 1. Firstly, the minimum energy required to complete a mission is independent of the range. On top of the optimized energy case on the design mission plus the battery energy neutral-expenditure possibilities, this concept is also able to complete two hops of 150 nm under the constraint of ground recharge. Results have shown that this concept is able to complete different types of scenarios with different objectives for the mission: whether it is to optimize the fuel burn, or, have a net battery energy expenditure equal to zero. This could be investigated even more to get an electrically self-sufficient aircraft with optimized fuel consumption and acceptable time impact depending on the operational context of the aircraft. This new function could be an improvement of the already existing Flight Management System that integrates a new input: State-of-Charge of the battery pack.

Significant improvements in terms of fuel burn reduction are obtained with the ARCH 4 concept. As has been stated in Ref. [2], this outcome can be explained by an increase in the overall propulsion system efficiency by virtue of increasing $H_{P,use}$. Together with a favorable L/D effect, which is proportional to aircraft weight increase, an improved ESAR outcome generates an overall energy expenditure benefit.

Upon completion of this exercise, the authors recommend a future VJB aircraft with a suitably flexible hybrid-electric architecture incorporating attributes of ARCH 4 (to permit significant emission reduction) and ARCH 1 (to permit dispatch under all circumstances) could be fashioned allowing possibility for the aircraft to complete any required city-pair operations (within the legitimate payload-range working capacity) irrespective of exchangeable batteries being available at a given station.

A sensitivity study was conducted assuming variation in kerosene price. It was deemed from the outset any variation in kerosene price from the nominal value, i.e. USD3.30 per USG, the nominal electrical energy price of USD0.1109 per kWh would remain fixed. This assumption was drawn by taking an analogue of studies presented in [37]. For ARCH 1 and ARCH 4, recalling the lower threshold of USD2.00 per USG for kerosene, 1-3% higher relative COC was found to occur. An increase to USG6.00 per USG for kerosene

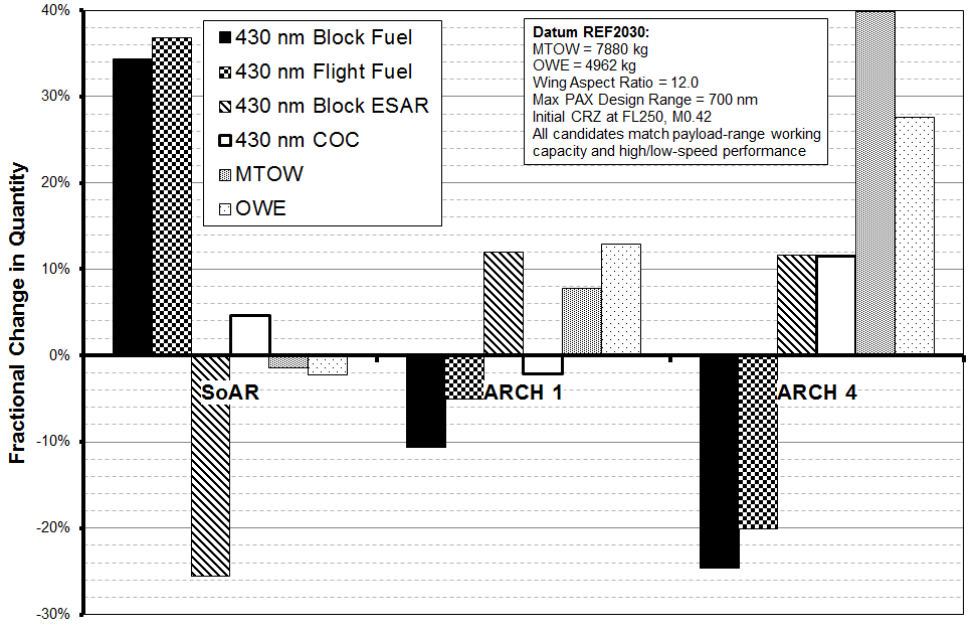

Fig. 14: Review of SoAR and design candidates versus the REF2030 (datum) aircraft

Tab. 6: VJB based aircraft design for 85-percentile stage length, Max PAX

Datum for VJB Design	Cell Batt. E Density (Wh/kg)	$H_{P,use}$ (-)	H_E (-)	$\triangleleft\eta$ (%)	$\triangleleft L/D$ (%)	$\triangleleft W_{ENR}$ (%)	$\triangleleft W_{PPS}$ (%)	$\triangleleft OWE$ (%)	$\triangleleft MTOW$ (%)	$\triangleleft$Block Fuel (%)
19 PAX **REF2030**	~800*	0.403	0.156	+40.3	+11.2	+256	+70.1	+27.6	+39.8	-20.1** 430 nm
70 PAX **PGT070*** **	910	0.510	0.128	+38.9	+7.8	+249	+126	+34.3	+51.2	-15.0 900 nm
180 PAX **PGT180*** **	940	0.474	0.144	+35.3	+5.6	+249	+101	+24.2	+35.9	-15.0 1100 nm

* Estimated based upon assumptions for design life, ageing effects, target state-of-charge and sensing requirements
** Flight fuel quoted instead due to much larger ratio of ground maneuvering allowance to block fuel
*** Data gleaned from Ref. [2]

resulted in 1-5% lower relative COC compared to Tab. 5. This indicates a significant impact of changes in kerosene price.

4.2 Benchmark against Previous Efforts

Table 6 above presents numerical particulars associated with the ARCH 4 design undertaken in this study as well as those published in Ref. [2]. Both the 70 and 180 PAX VJB aircraft concepts employ tri-fan (two under-wing podded gas-turbines and one aft-fuselage mounted, S-duct configured electrically driven motor) morphologies with corresponding typical cruise speeds of M0.75-76. In addition, taxi-in/out were assumed to be performed using gas-turbines only for the 70 PAX and 180 PAX VJB aircraft as opposed to the 19 PAX VJB, which employs electrically powered ground maneuvering. Furthermore, all candidates presented in Tab. 6 utilize Normal Conducting Machines delivering shaft power output of 1.1 MW, 4.5 MW and 8.5 MW for the 19 PAX, 70 PAX and 180 PAX respectively.

All aircraft presented in Tab. 6 share a common analysis methodology for operating economics and are characterized by a $\triangleleft$COC result of around +10%. As posed in Ref. [2] a challenge to the industrial and academic engineering communities was made in seeking ways to decrease the specific weights of electrical sub-systems/components as well as ameliorating the VJB DMC impact is necessary in securing an overall cost neutral outcome. Assuming 85-percentile stage lengths, for

similar battery cell-level energy densities and block fuel outcome of 15-20% reduction it can be readily observed that a striking similarity in parametric values occurs irrespective of scale effect and mission role (passenger accommodation and flight technique): common values of $H_{P,use}$ = 0.40-0.51 and H_E = 0.12-0.16 appear evident. Furthermore, it can be seen these parametric descriptor values tend to generate quite similar values in ◁MTOW, ◁OWE, Release Energy Weight (◁W_{ENR}, includes both block and reserves-contingency) and PPS Weight (◁W_{PPS}).

5 Conclusion

This technical paper focused on setting technical targets for a future 19-passenger commuter aircraft employing hybrid-electric, battery based Voltaic-Joule/Brayton (VJB) motive power systems with no additional electrical energy drawn from generators mechanically coupled to thermal engines. The adopted morphological solution was a tri-prop comprising two on-wing podded turbo-props and one aft-fuselage mounted electric motor configured as a pusher-on-pylon installation. Assuming a Battery System-level Gravimetric Specific Energy (referred to as "battery energy density") of at least 500 Wh/kg block fuel reduction of up to 39%, 25% and 10% for 150 nm (Design Service Goal), 430 nm (85-percentile) and 700 nm (maximum range) stage lengths respectively could be realised. All utilize electrically powered ground maneuvering and quoted comparisons are against a suitably projected turbo-prop only year-2030 aircraft. From a Cash Operating Cost perspective, all investigated stage lengths were predicted to be around 8-14% higher relative to the datum of a projected turbo-prop only year-2030 aircraft. Upon comparison of this 19 PAX VJB to previously studied 70-passenger and 180-passenger VJB concepts a common theme of Degree-of-Hybridization for Useful Power, $H_{P,use}$ = 0.40-0.50, and, Degree-of-Hybridisation for Stored Energy, H_E = 0.120-0.150, for a given block fuel outcome of 15-20% reduction appeared evident.

6 Acknowledgments

Gratitude is conveyed to the following individuals for their contributions to the analysis and work presented in this paper:

- Aurelie Boisard, SAFRAN S.A.
- Gäetan Chesneau, SAFRAN S.A.
- Radu Cirligeanu, SAFRAN S.A.
- Anthony Gimeno, SAFRAN S.A.
- Nawal Jaljal, SAFRAN S.A.
- Hugo Jouan, ISAE-SUPAERO Intern
- Julien Labbe, SAFRAN S.A.
- Pierre-Alain Lambert, SAFRAN S.A.
- Samer Maalouf, SAFRAN S.A.
- René Meunier, SAFRAN S.A.
- Benoit Rodriguez, SAFRAN S.A.
- Arturo Santa Ruiz, Georgia Tech Intern
- Andy Turnbull, SAFRAN S.A.

References

[1] Advisory Council for Aviation Research and Innovation in Europe (ACARE), "*Realising Europe's Vision for Aviation: Strategic Research and Innovation Agenda, Volume 1*", September 2012.

[2] Isikveren, AT, Pornet, C, Vratny, PC, Schmidt, M, "Optimization of Commercial Aircraft Utilizing Battery-based Voltaic-Joule/Brayton Propulsion", *AIAA Journal of Aircraft*, DOI 10.2514/1.C033885, accepted for publication, 2016.

[3] Pornet, C, Isikveren, AT, "Conceptual Design of Hybrid-Electric Transport Aircraft", *Progress in Aerospace Sciences*, Vol. 79, pp. 114–135, DOI: 10.1016/j.paerosci.2015.009.002, 2015.

[4] Pornet, C, "Electric Drives for Propulsion System of Transport Aircraft", book chapter, "*New Applications of Electric Drives*", Chomat, M (Editor), ISBN 978-953-51-4603-2, InTech, 2015.

[5] Isikveren, AT, Kaiser, S, Pornet, C, Vratny, PC, "Pre-design Strategies and Sizing Techniques for Dual-Energy Aircraft", *Aircraft Engineering and Aerospace Technology Journal*, Vol. 86, Issue 6, DOI: 10.1108/AEAT-08-2014-0122, 2014.

[6] Pornet, C, Kaiser, S, Isikveren, AT, and Hornung, M, "Integrated Fuel-Battery Hybrid for a Narrow-Body Sized Transport Aircraft", *Aircraft Engineering and Aerospace Technology Journal*, Vol. 86, Iss. 6, pp. 568-574, DOI 10.1108/AEAT-05-2014-0062, 2014.

[7] Pornet, C, Gologan, C, Vratny, PC, Seitz, A, Schmitz, O, Isikveren, AT and Hornung, M, "Methodology for Sizing and Performance Assessment of Hybrid Energy Aircraft", *AIAA Journal of Aircraft*, Vol. 52, No. 1, pp. 341-352, DOI 10.2514/1.C032716, 2015.

[8] Bradley, MK, Droney, CK, "*Subsonic Ultra Green Aircraft Research : Phase I Final Report*", Huntington Beach, California, 2011.

[9] Banning, T, Bristow, G, Level, C, Sollmann, L, Calderon-Fernandez, J, Wells, D, Olson, M, Davis, N, Du, C, Ambadpudi, S, "*2012-2013 FAA Design Competition for Universities Electric / Hybrid-Electric Aircraft Technology Design Category - NXG-50*", Georgia Tech, USA, 2013.

[10] Miller, P, "Potential Propulsion Solutions for Hybrid-Electric Aircraft", *Disruptive Green Propulsion Technologies Conference, Institute of Mechanical Engineers*, London, United Kingdom, 2014.

[11] Isikveren, AT, "Design and Optimisation of a 19 Passenger Turbofan Regional Transport", Paper 1999-01-5579, *1999 SAE World Aviation Congress*, San Francisco, California, USA, October 1999.

[12] PT6A Cutaway, http://www.keyword-suggestions.com/cHQ2YSBjdXRhd2F5/, accessed 06 July 2016.

[13] PROOSIS, Propulsion Object-Oriented Simulation Software,http://www.ecosimpro.com/products/proosis/, accessed 06 July 2016.

[14] Type Certificate Data Sheet E26NE, Pratt and Whitney, US Department of Transportation, *Federal Aviation Administration*, Rev. 14, 04 November, 2011.

[15] 2002 Aerospace Source Book, *Aviation Week & Space Technology*, Vol. 156, No. 2 McGraw-Hill, 14 January, 2002.

[16] Jane's All the Worlds Aircraft 2001-2002.

[17] Jane's Aero-Engines 2000.

[18] Flight International World Aircraft & Systems Directory, Third Edition, *Flight International*, 2002.

[19] Isikveren, AT, Seitz, A, Bijewitz, J, Mirzoyan, A, Isyanov, A, Grenon, R, Atinault, O, Godard, J-L, Stückl, S, "Distributed Propulsion and Ultra-high By-Pass Rotor Study at Aircraft Level", *The Aeronautical Journal*, Vol. 119, No. 1221, pp.1327-1376, 2015.

[20] Mistree, F, Lewis, K, Stonis, L, "Selection in the Conceptual Design of Aircraft", AIAA-94-4382-CP, *32nd AIAA Aerospace Sciences Meeting and Exhibit*, Reno, NV, January 10-13, 1994.

[21] Brown, G. V., "Weights and Efficiencies of Electric Components of a Turboelectric Aircraft Propulsion System", AIAA 2011-225, *49th AIAA Aerospace Sciences Meeting including the New Horizons Forum and Aerospace Exposition*, Orlando, FL, USA, 2011.

[22] Galea, M, "Aerospace Machines and Drives – Towards More Power Density, Reliability and Efficiency", *Electric and Hybrid Aerospace*, 2015.

[23] Barchasz, C, "*Développement d'accumulateurs Li/S*", PhD Thesis, Université de Grenoble, 25 October 2011.

[24] Piancastelli, L, Pellegrini, M, "The Bonus of Aircraft Piston Engines, An update of the Meredith Effect", *International Journal of Heat and Technology*, Vol. 25, No. 2, pp. 51-65, 2007.

[25] Association of European Airlines (AEA), "*Operating Economy of AEA Airlines*", 2007.

[26] Transport Studies Group (TSG), "*Aircraft Crewing - Marginal Delay Costs*", London, United Kingdom, 2008.

[27] Aircraft Operating Costs and Statistics Turboprop Aircraft, Market Briefing, p. 7, *Aviation Week Intelligence Network*, 16 July 2012.

[28] Plötner, KO, Wesseler, P, Phleps, P, "Identification of Key Aircraft and Operational Parameters Affecting Airport Charges", *International Journal of Aviation Management*, Vol. 2, No. 1/2, pp. 91-115, 2013.

[29] Khan, K, Houston, G, "*Design Optimization using Life Cycle Cost Analysis for Low Operating Costs*", Bombardier Aerospace, Ontario, Canada, 2000.

[30] Rupp, OC, "*Vorhersage von Instandhaltungskosten bei der Auslegung ziviler Strahltriebwerke*", Dissertation, Technical University of Munich, Germany, 2000.

[31] Majeed, O, "*Beechcraft 1900D: Fuel, Emissions & Cost Savings Operational Analysis*", Document Ref: SRS-TSD-007 Rev. 0, 21 February 2012.

[32] http://compair.aviationresearch.com/pdf.aspx?action=print_aircraft_report&id=412&document_id=3, accessed 24 June 2016.

[33] http://www.eia.gov/dnav/pet/hist/LeafHandler.ashx?n=PET&s=EER_EPJK_PF4_RGC_DPG&f=D, accessed 15 September 2014.

[34] Baranowski, D, "*Development of an Operating Cost Model for Electric-Powered Transport Aircraft*", Diploma Thesis, Technical University of Munich, Munich, Germany, 2012.

[35] https://www.pace.de/products/design.html, accessed 23 February 2016.

[36] http://www.openvsp.org/, accessed 19 March 2016.

[37] http://www.eei.org/ourissues/EnergyEfficiency/Documents/Prices_graph_2012.pdf, accessed November 2014.

Copyright Statement